Metrol. Meas. Syst., Vol. 30 (2023) No. 4, pp. 689–702
DOI: 10.24425/mms.2023.147959

PAN POLSKA AKADEMIA NAUK

METROLOGY AND MEASUREMENT SYSTEMS
Index 330930, ISSN 0860-8229
www.metrology.wat.edu.pl

M&MS

A GRINDING SURFACE ROUGHNESS CLASS RECOGNITION COMBINING RED AND GREEN INFORMATION

Jiefeng Huang[1,2)], Huaian Yi[1,2)], Runji Fang[1,2)], Kun Song[1,2)]

1) Key Laboratory of Advanced Manufacturing and Automation Technology (Guilin University of Technology), Guilin, China, 541006 (1426281214@qq.com, ✉ yihuaian@126.com, 1318371594@qq.com, 546345784@qq.com)
2) School of Mechanical and Control Engineering, Guilin University of Technology, Guilin, China, 541006

Abstract

The current machine vision-based surface roughness measurement mainly relies on the design of feature indicators associated with roughness to measure the surface roughness. However, the process is tedious and complicated. Moreover, most existing deep learning methods for workpiece surface roughness measurement use a monochromatic light source to acquire images. In the case of surface roughness in a grinding process with low roughness and random texture characteristics, the feature information obtained by monochromatic light source acquisition is relatively small. It is difficult to extract the workpiece surface roughness features, which can easily cause problems for subsequent measurement. Based on the problems above, this paper proposes a grinding surface roughness measurement method combining red-green information and a convolutional neural network. The technique uses a particular red-green block to highlight the grinding surface texture features. Finally, it classifies the grinding surface roughness measurement with a classification detection technique of the convolutional neural network. Experimental results show that the accuracy of the grinding surface roughness measurement method combining red-green information and the convolutional neural network is significantly improved compared with that of the grinding surface roughness measurement method without using the red-green data.

Keywords: roughness measurement, convolutional neural network, red and green information.

1. Introduction

Workpiece surface roughness affects the performance of parts, in terms of *e.g.* their service life and reliability, and is one of the critical parameters used to measure the quality of workpiece processing. Traditional workpiece surface roughness measurement is generally measured by contact and is achieved with a diamond stylus. Regrettably, with this method it is easy to scratch the measured surface, and the efficiency of the measurement is low. It can only be applied to accurate measurement of some surface profile roughness and online measurements [1]. Therefore, some researchers have developed many non-contact optical measurements devices, such as white

Article history: received May 5, 2023; revised August 2, 2023; accepted August 16, 2023; available online November 19, 2023.

light interferometers, atomic force microscopes and laser microscopy systems. However, the devices are limited in engineering applications by prohibitive costs, strong influence of the work conditions, and the limited measurement field of view.

To overcome the limitations of traditional mechanical measurement, workpiece surface roughness measurement based on machine vision has begun to be widely used. Machine vision measurement is based on the principle of optical imaging which uses industrial cameras to capture images of the workpiece surface and then extracts the feature indicators in the photos associated with surface roughness values. Finally, it predicts surface roughness at the location corresponding to the known image feature indicators. Chen [2] multi-feature descriptors are constructed by speckle features, grayscale features and Tamura texture features. Then, an *accuracy* (ACC) random forest-based recognition inference method is proposed to determine the classification of artifacts. In order to predict the roughness of the workpiece surface, Dhiren [3] established a correlation between the *two-dimensional* (2D) surface roughness parameters and the part texture features, with which the texture features were extracted by the *Gray Level Co-occurrence Matrix Algorithm* (GLCM) and a machine vision system to enable the prediction of surface roughness. All the methods above for predicting surface roughness based on feature metrics binarize the images and thus extract grey information features. Still, the grayscale map has less feature information and cannot characterize the workpiece surface roughness well, leading to incorrect prediction of the workpiece surface roughness.

To fully exploit the color information features, Yi [4] proposed that the surface roughness of a ground part is examined by the quality of the virtual image formed by a color pattern on the surface of the ground part. The color pattern can be regarded as a reference, and the surface roughness of the specimen is judged according to the change in the clarity of its virtual image on the surface of the sample. Yi [5] proposed a roughness detection method based on the average color difference index of the color difference mechanism which predicts the surface roughness by means of a regression model of a support vector machine. Liu [6] proposed a statistical matrix of color distribution based on red-green spatial information and the corresponding overlap index, and established metrics thus enabling the prediction of surface roughness. Lu *et al.* [7], proposed a color image-based metric design and an evaluation method to model the correspondence with roughness. All the methods above make a fuller use of color information. Still, the feature indices of the techniques above are designed by humans and extracted manually. The operation process is tedious and more vulnerable to human disturbance, which is unsuitable for industrial automation in measuring the surface roughness of workpieces. When the predicted roughness range grade is high, errors may occur.

With the development of artificial intelligence in recent years, deep learning-based methods have also been applied to workpiece surface roughness assessment. Rifai *et al.* [8] preprocessed the obtained images to enhance the texture features of the workpiece surface. They used convolutional neural networks to predict the workpiece surface roughness directly from digital surface texture images, avoiding the disturbance caused by artificial extraction of characteristics. SAEEDI *et al.* [9] used a convolutional neural network as a regressor and classifier to classify steel surface roughness, which is faster and more adaptable compared to traditional methods for automatic feature extraction. Leonie Tatzel *et al.* [10] trained a *convolutional neural network* (CNN) on a database containing a large number of images and corresponding roughness values to achieve roughness measurements of laser-cut stainless-steel edges by means of RGB images rather than surface topography. Chen *et al.* [11] used an end-to-end image analysis approach to achieve different grades of milled surface roughness classification using the Xception model with a small number of source images pre-processed with image enhancement in two experimental light source environments with different brightness during day and night. Giusti [12] proposed a machine-

integrated inexpensive optical measurement system based on convolutional neural networks, which measured Ra values comparable to the results of a contact profilometer and had the potential to provide more information about the surface topography. Ibarra-Zarate [13] proposed a roughness characterization through acoustic emission followed by roughness measurement by classification models. Qi [14] used an improved Mahalanobis distance and a CNN method to build a multilayer model for grinding condition classification and recognizing distinct wear stages of abrasive belts. The roughness measurement methods described above for automatic feature extraction are faster and more adaptable than the traditional feature extraction methods without human interference. However, most of the image acquisition techniques above use monochromatic light sources. For grinding processes, the roughness texture information of the workpiece surface obtained using monochromatic light source imaging is weak, which will cause problems for subsequent feature extraction.

To deal with the mentioned difficulties, this paper proposes a grinding surface roughness measurement method combining red and green information, which uses a customized red-green block. In this method, when light is mirrored to the surface of the working piece through the red-green combination, *i.e.* the light changes to red and green, forming a dummy image on the workpiece surface, and then the camera captures the picture. From [4, 5], it can be known that combining the red and green information and then acquiring the images can highlight the texture features of the workpiece on the grinding surface better and finally connect with the convolutional neural network to automatically extract the elements. Thus, the surface roughness of the workpiece can be predicted accurately and quickly. This method can highlight the surface texture features of the workpiece without the need for artificially designed feature indicators and, at the same time, provides a basis for online roughness detection in industrial automation.

The remaining part of the article is devised as follows: Section 2 introduces the principle of rough surface imaging, the red-green letter-based rough surface imaging method, and the convolutional neural network model used for grinding surface roughness grade prediction. Section 3 introduces the experimental processes and comparison experiments, Section 4 analyses the experimental results, Section 5 concludes, and Section 6 summarizes the article.

2. Methods

2.1. Rough surface imaging

Visual imaging is related to the reflection of light. When light shines on the target object, it is reflected in a mirror, and plane lens in turn reflects the light back into the eye of the human being, at which time we can see the virtual image formed by the target object on the plane mirror. In the same way, when the rough surface of the grinding workpiece is imaged, the grinding workpiece is regarded as a plane mirror and the industrial camera is viewed as the human eye. A target M is selected, the industrial camera can capture the virtual image of the target formed on the grinding surface [3]. The whole imaging process is shown in Fig. 1 below.

When the light source shines on the surface of the target M and then reflects, at this time, the target M can be considered as a point light source. Suppose two beams of light from point M, after mirror reflection, the incident light forms M concentrated at the same point M1′; when the camera focal length is appropriate, the camera imaging surface captures an obvious moment M1″, as shown in Fig. 1(a).

The surface of the grinding workpiece being uneven causes the light beam from M to be diffusely reflected by the rough surface of the grinding workpiece, and part of the light will enter

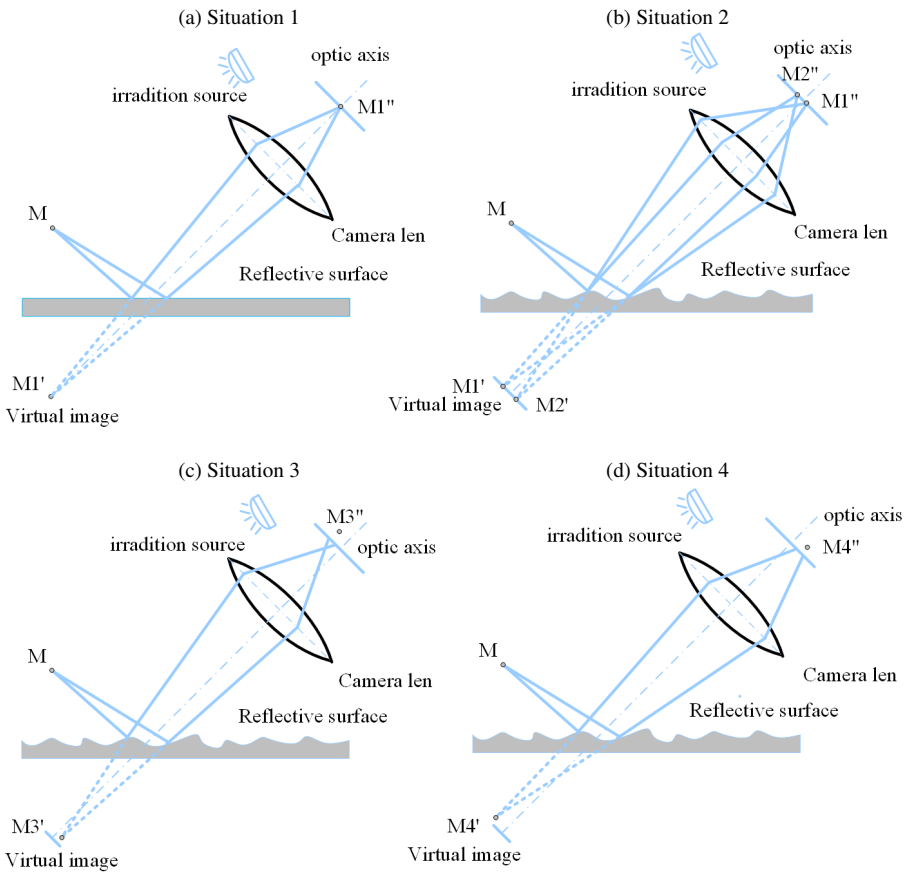

Fig. 1. Imaging under different reflective surface conditions.

the camera's shooting area, resulting in the situation shown in Fig. 1(b). When the camera's focal length is fixed, the light reflected by the rough surface enters the camera exactly when it is focused on the camera imaging surface, producing a clear point. As diffuse reflection from the rough surface occurs, multiple false images are formed at the same moment, and the reflected light passes through the camera lens without focusing on the camera imaging surface. Fig. 1(c) and 1(d) show the reflected light focus in front of and behind the imaging surface, respectively. It will become a blurred point, and the image transmitted by the camera will likewise become blurred [15].

Thus, the quality of imaging is related to the location of the focus point and the amount of light reflected into the camera, and the quality of the target object imaged on each rough surface is related to the light intensity and surface properties, *etc*. [16]:

$$I(ij) = f\big(L(ij), R(ij), S(ij)\big). \tag{1}$$

In the formula above, the single-pixel positions are noted as (ij), $i = 1, 2, \ldots, M$, $j = 1, 2, \ldots, N$, $M \times N$ is the image range. $L(i, j)$ is the intensity of light indicates the intensity of light and the amount of surface area of an object being illuminated. $R(i, j)$ is the rough surface that can

reflect light. Different materials have different optical properties and have different reflectance on their surface, thus $S(i, j)$ are the surface properties of the material, including material roughness and surface texture direction, *etc*. [17].

2.2. Rough surface imaging based on red-green blocks

As can be seen from 2.1, the imaging situation is different for different reflective surfaces. From the literature [5] we can learn that when we replace the target in Fig. 1 above with a red-green block, the absolute value of the red-green difference per point pixel of the color image is monotonically related to the roughness, *i.e*., the total value of the red-green difference per point pixel of the virtual image of the smooth surface is more significant than that of the rough surface. It indicates that the grinding surface roughness can be turned into an image using the red-green block, and the grinding surface features can be enhanced in the red-green blended area of the imaging.

However, when we use a convolutional neural network to recognize and classify the grinding surface roughness directly, classification accuracy needs to be improved because the texture of the grinding surface is random and the features are weak. Therefore, we use the red-green block to highlight the texture features of the grinding surface and regard the red-green block as the target. When the white light source is irradiated on the red-green block, the light source reflected by the red-green block has red and green double colors, at this time, the red-green block can be regarded as a particular red-green light source, and the double-colored light source reflected by the red-green block is irradiated on the surface of the grinding workpiece and finally reflected into the camera image by the grinding surface.

2.3. Convolutional neural network structure introduction

In this paper, the VGG16 model [18] is used to extract features for grinding surface roughness and thus for classification. That is, the image is input to VGG16 on the convolutional neural network, through the internal convolution operation of the convolutional layer. The principle of the convolutional layer to extract features is calculated as follows: Equation (2), where the k convolutional kernel of layer i forms the feature map defined as the weight matrix is W_i^k, the bias is denoted as b_i^k, $\otimes$ denotes the dot product, and f is the activation function.

$$F_i^k = fW_i^k \otimes F_{i-1}^k + b_i^k, \qquad i = 1, 2, \ldots, N. \tag{2}$$

The output of the convolutional layer is used as the input of the pooling layer, which is equivalent to downsampling [19], and allows feature downsampling and feature extraction of the input sample images. The pooling layer divides the input into non-overlapping blocks, and then features are extracted from each region. Where the feature maps formed by the k convolution kernels of layers, i and $i-1$ are denoted as F_i^k and F_{i-1}^k, the bias is denoted as b_i^k, C is the downsampling style, and f is the activation function, which is calculated as follows:

$$F_i^k = f(C(F_{i-1}^k) + b_i^k), \quad i = 1, 2, \ldots N \tag{3}$$

The VGG16 model uses a 2×2 maximum pooling layer for spatial downsampling, reducing the size of the feature map by half [19], which optimizes the VGG16 model by compressing the data and parameters and preventing overfitting of the model training. The last one is the fully connected layer, which classifies the input sample images relevant to the extracted features. This

classification is achieved by adjusting the final output layer of VGG16 according to the category of the actual grinding sample images for grinding surface roughness.

The process of classifying grinding surface roughness using the VGG16 model is shown in Fig. 2 below, and the input image size of the VGG16 convolutional neural network model is $224 \times 224 \times 3$, in which the model has a total of 13 convolutional layers and 3 fully connected layers [20]. The classification process of grinding surface roughness is as follows: firstly, the grinding surface image combining red and green information is subjected to feature extraction by the convolutional kernel. Next, feature dimensionality reduction is performed by the pooling layer, and then the grinding surface roughness images is output by the fully connected layer to achieve the classification of the input grinding surface roughness image.

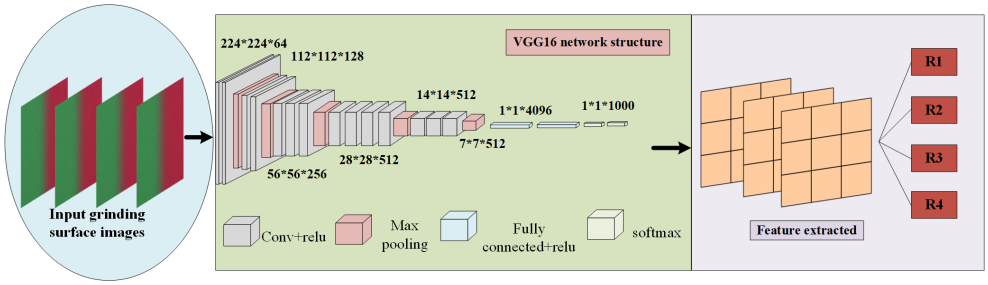

Fig. 2. Grinding surface roughness classification process.

3. Experiment

With a view to examine the grinding surface roughness method combining red-green information and convolutional neural network, this paper explores the effect of the technique on the recognition of grinding surface roughness grades through comparative experiments, and the experimental steps are shown in Fig. 3 below. First, the 45 steel grinding workpiece with different

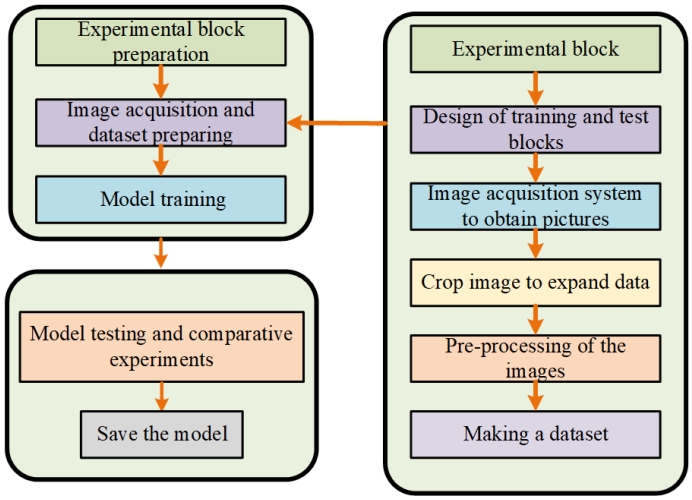

Fig. 3. Flow of experimental steps.

roughness was processed by a grinder and divided into roughness classes. Then, a particular red-green block captured the images of the machined workpieces, and a dataset was created. Finally, the produced grinding dataset was divided into training and test sets, and the trained model was saved and tested for its effectiveness in grinding surface roughness recognition.

3.1. Sample preparation

Considering that is easy to grind and has good reflective properties for subsequent machine vision inspection of roughness, in this study 45 steel was used to fabricate the sample blocks for experimental research. The grinding sample was machined using a manual surface grinder HR-618S with a model 1 200 × 16 × 32 WA 120 K 5 V 35 m/s white corundum grinding wheel, with a size of 50 mm. By changing the grinding parameters such as grinding wheel speed, workpiece speed and depth of cut, the grinding sample with different roughness was machined and used as the experimental workpiece.

During the actual machining process, the roughness is not the same at all locations on the same machined surface, so users are more concerned about the roughness of the workpiece surface during the process. Our research mimics the ISO roughness grade standard, considering the true roughness value range of the grinding sample block; the roughness classification is designed as 4 classes, where the first grade of roughness ranges from (0–0.3) μm and is labeled R1, the roughness second-grade range is (0.3–0.8) μm and is labeled R2, the third level of roughness ranges from (0.8–1.6) μm and is denoted as R3, and the fourth roughness class range is (1.6–2.4) μm as R4, and the processed sample blocks and roughness range statistics are shown in Table 1 below.

3.2. Image Acquisition and dataset production

The structure of the device for grinding specimen surface roughness image acquisition is shown in Fig. 4(a) below. The grinding specimen inspection surface is perpendicular to the table, the color block is at an angle of 45° to the table as shown in Fig. 4(b) below, and the camera is parallel to the red-green block. When the white strip light source shines on the red-green block (150 mm × 150 mm), it is reflected on the surface of the workpiece through the color block. At this time, the light source becomes red and green and then demonstrates the camera image through the surface of the workpiece. Thus, the camera acquires an image that is perpendicular to the camera's optical axis and is a virtual image of the color block. During the experiment, the light source environment is controlled, the camera and color block positions are fixed, and the grinding specimen is fixed to the iron plate with a magnet. The light source was a white OPT-LI21222 LED with an OPT-DPA1024E-4 light source controller, and the light intensity was

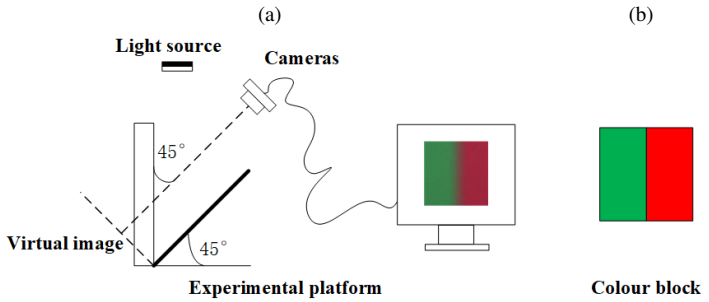

Fig. 4. Image acquisition device.

measured using a TES-1335 light meter. The digital images were captured and stored via a data cable controlled by the Pylon 4 software installed on the computer.

The workpiece with different grades of roughness was photographed using an image acquisition device, as shown in Fig. 5 below. Figure 5(a) shows the first grade of roughness, Fig. 5(b) shows the second grade of roughness, and Fig. 5(c) shows the third grade of roughness. As the grade of roughness becomes more extensive, the surface features of the virtual image formed on the workpiece through the red-green block become more prominent, and for the convenience of the present study, the obtained grinding surface sample roughness images are cropped to obtain the pixel size of 224×224, and the obtained grinding surface roughness sample images are made into a data set, of which 75% is the training set of the samples, and 25% is the validation set of the samples.

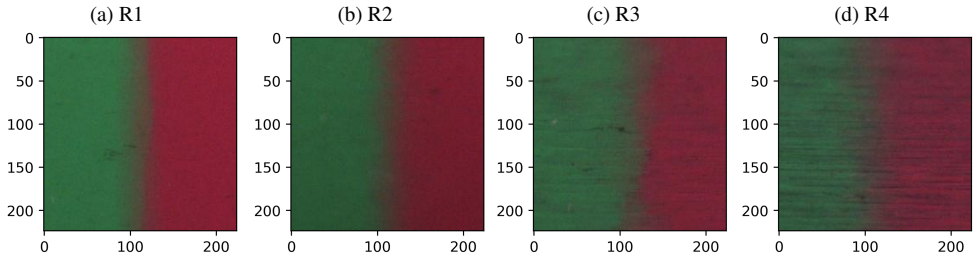

Fig. 5. Image of the grinding surface obtained by the image acquisition device.

Due to the application of the deep learning-based grinding surface roughness detection method, a large number of samples are required to train the model, a grinding dataset is produced and the obtained grinding surface images will be used to expand the data using data enhancement methods (panning, rotating, cropping, *etc*.) and the data enhanced grinding surface images are assembled into a dataset as well to improve the model's ability to generalize and to reduce the model's sensitivity to the input images. The final dataset will be produced demonstrated as listed in Table 1 below.

Table 1. Classification and number statistics of samples.

Roughness (μm)		**R1 (0–0.3)**	**R2 (0.3–0.8)**	**R3 (0.8–1.6)**	**R4 (1.6–2.4)**	**Total**
Training set	Before data enhancement	160	120	160	140	580
	After data enhancement	800	600	800	700	2900
Test set		40	40	40	40	160

3.3. Model Training

In this paper, the VGG16 network model is calibrated to achieve grinding surface roughness classification by fine-tuning its final output layer categories into four categories and determining the parameters of the model through pre-experiments. The image dataset was pre-processed to expand the samples in order to increase the generalization ability of the model. Then the dataset was input into the model and the features were automatically extracted from the input images by the feature extraction structure of the VGG16 network The extracted features were then downscaled

by the fully connected layer features, and finally, the classifier is used to accomplish the class classification of grinding surface roughness.

With the learning rate of the model set to 0.01, the batch size set to 16, and the Adam optimizer selected to update the model network parameters, the model was trained and tested under the Windows 11 operating system with the hardware parameters and the deep learning frame used as shown in Table 2 below.

Table 2. Hardware parameters and the deep learning framework used.

Name	Configuration
Operating System	Windows 11
CPU	Intel(R) Core^{TM} i5-12400F
GPU	GeForce GTX 3050
Deep Learning Framework	Tensorflow 2.6.0

3.4. Model test comparison experiment

Firstly, in order to demonstrate the effectiveness of self-feature extraction for grinding surface roughness measurement, we trained the roughness images with combined red and green information using the VGG16 model and extracted the red and green components from the obtained grinding surface roughness dataset images through image processing. The photos were displayed as shown in Fig. 6 below and the grinding surface roughness images without red and green information were obtained. The same model was selected to train the classification and the obtained results are compared.

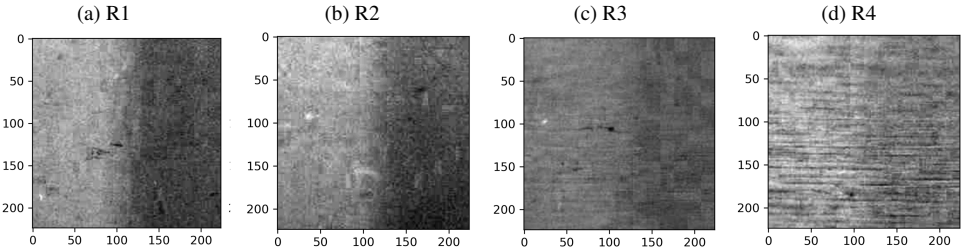

Fig. 6. Image of the grinding surface without red and green information.

Also, for the comparison of the grinding surface roughness measurement method with manual characteristic extraction and the measurement method with self-feature extraction, the prediction results of a support vector machine (SVM) based on CD metrics were used for comparison as a measure of the validity of the grinding surface roughness measurement method combining red and green information with convolutional neural networks.

4. Analysis of experimental results

4.1. Analysis of grinding surface roughness measurement results with self-extracted features

Firstly, for analyzing the roughness classification model with self-feature extraction, the measurement results of the roughness sample images with combined red and green information

fed into the VGG16 network training are compared with the roughness sample images without red and green information, as shown in Fig. 7 below. Figure 7(a) shows combining red and green data proving that the classification accuracy reaches 95%, and the model line training process loss values gradually converge. Figure 7(b) shows the classification results of the grinding surface roughness sample images without combining the red and green information. From the results, the classification of the grinding surface roughness images without combining the red and green information is not adequate, the accuracy rate is only about 25%, and the loss value does not converge during the model training process, it is always in oscillation, and the loss value is large.

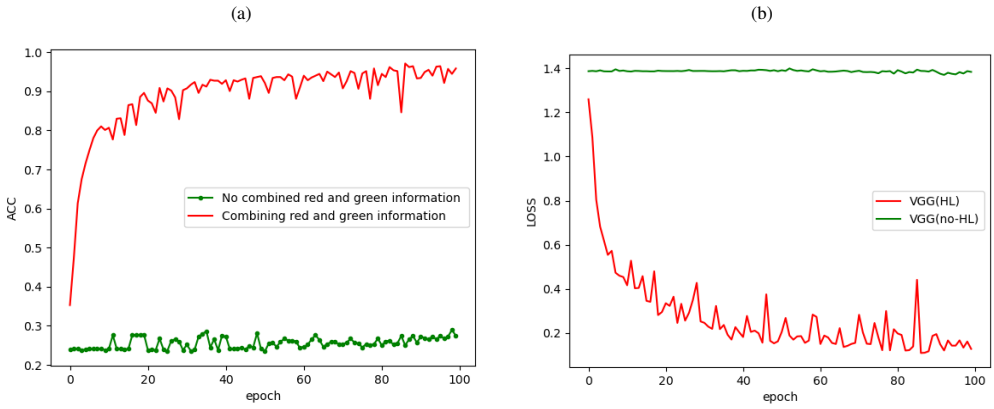

Fig. 7. Classification accuracy and loss value.

The trained model was also tested and the confusion matrix of the test results was made, as shown in Fig. 8 below. Figure 8(a) shows the test with the model trained with combined red and green information, and Fig. 8(b) shows the test results of the model trained without combined red and green information. Due to the relatively small surface roughness of the ground workpiece and the random irregularity of the surface texture, the surface texture information without combining

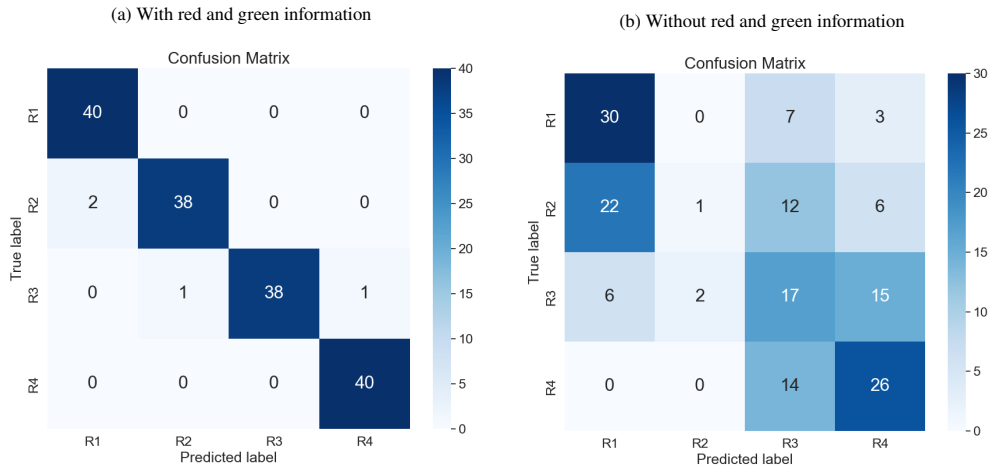

Fig. 8. Confusion matrix for classification results.

red and green information is weak, and the recognition effect of the individual categories is poor. Because the surface texture of grinding processing is more random, the above experimental data showed that combining red and green information could improve the recognition of grinding surface roughness. The texture features of the grinding surface with combined red and green information are more prominent and easier to recognize when the neural network extracts the features.

4.2. Analysis of grinding surface roughness measurement results with manually extracted features

For the grinding surface roughness measurement with manual feature extraction, the results of SVM classification based on CD metrics are shown in Fig. 9(a) below. The effects of SVM (Gray SVM) classification based on grayscale co-occurrence matrix are shown in Fig. 9(b) below. We can see in the Fig. 9 below that the effect of using artificial methods for feature extraction and recognition measurement is poor, and the recognition was worse in all four categories The classification situation is poor in all four types. This indicates that the artificial feature extraction method is ineffective in recognizing and measuring grinding surface roughness.

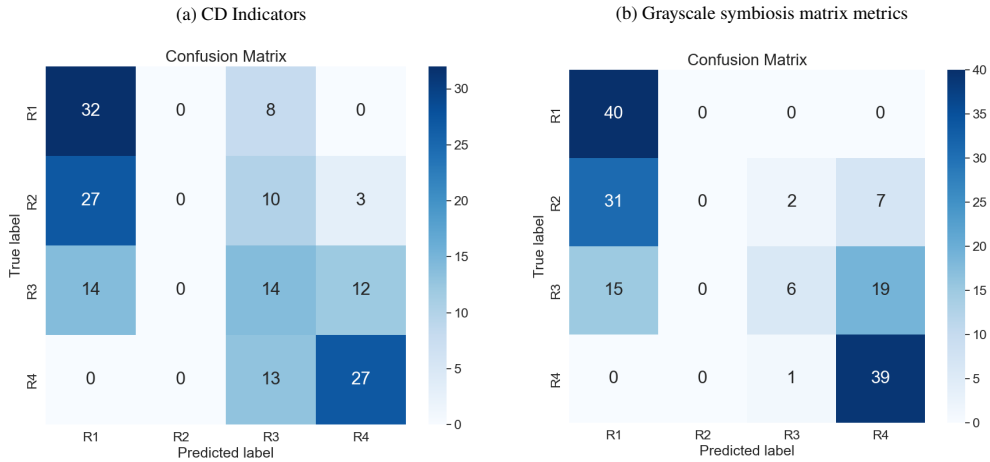

Fig. 9. Matrix metrics.

In addition, we calculated the accuracy, precision, and recall of each model, and the resulting confusion matrix is presented in Table 3 below.

Table 3. Accuracy of each classification model.

Models	Precision	Recall	Accuracy
VGG (with red and green information)	97.56%	97.50%	98.75%
VGG (no red and green information)	49.74%	46.87%	76.42%
SVM(CD)	45.63%	45.63%	72.81%
SVM (grayscale co-occurrence matrix)	53.13%	53.13%	76.57%

For the recognition measurement method of feature extraction, the recognition accuracy of grinding surface roughness measurement combined with red and green information is higher, reaching 97.56%. However, the recognition accuracy of the self-extracted feature method with red and green information removed is only 49.74%, which means that combining red and green information can improve the efficiently of recognition accuracy of grinding surface roughness measurement. For the manually extracted recognition measurement method, the recognition accuracy based on CD indicators was only 45.63%, and the recognition accuracy with the grayscale covariance matrix was only 53.13%. From the analysis of the experimental results, we can see that the grinding surface roughness recognition measurement method combining red-green information and a convolutional neural network could efficiently address the problems of weak texture characteristics of the grinding surface, random texture and complex recognition.

5. Discussion

We made a scatter plot of the CD metric values under different illumination for this purpose, as shown in Fig. 9(b) below, indicating that the recognition measurement method based on deep learning feature self-extraction is more effective for the recognition of images with random texture and weak features such as ground machining surfaces.

Due to the fixed position of the camera, the light reflected from the grinding surface into the camera also differs depending on the placement of the grinding surface texture direction. When the workpiece surface texture direction is placed parallel to the table direction, the surface characteristics obtained by imaging a specific red-green block are different from the vertical table placement, and since the camera is placed 45°above the grinding workpiece when the workpiece surface texture direction is parallel to the table, the camera is rated at 45°above the grinding workpiece when the texture direction of the workpiece surface is similar to the table, the light reflection on the workpiece surface is up and down. More information is imaged in the camera than in the vertical table direction, so whether the grinding workpiece is placed properly or not has a more significant impact on the measurement of the grinding surface roughness.

Also, when light sources of different intensities are illuminated on the workpiece's surface, the camera's imaging results can vary. In environments with low light intensity, the light source images fewer features on the workpiece surface through the red and green blocks, which can interfere with subsequent identification. In a high-light-intensity environment, the image in the camera is more likely to have shadows, which also affects the subsequent roughness recognition measurement.

6. Conclusions

This paper proposes a method for grinding surface roughness measurement that combines red and green information. The method uses a customized red-green block, and when the light is reflected on the workpiece surface through the red-green filter, the light changes to red and green, forming a virtual image on the workpiece surface, which integrates the red and green information into pictures. These pictures can highlight the texture features of the grinding surface. It is finally combined with convolutional neural network automatic feature extraction, thanks to which its performance is accurate and quick. The surface roughness of the workpiece can be predicted accurately and promptly. The experimental results showed that, compared with the grinding surface roughness measurement method without red and green information, the accuracy of

the grinding surface roughness measurement method combining red and green information and convolutional neural network reached 97.56%, which was 47.82% higher than that of the grinding surface roughness classification method without red and green knowledge, 51.93% higher than that of the recognition method based on CD indicators, and 51.93% higher than that of the recognition method based on greyscale co-generation matrix indicators. The technique can highlight the texture features of the grinding workpiece surface and automatic feature extraction, avoiding feature extraction and eliminating the need to combine the machining process parameters, which provides the possibility to achieve visual classification measurement of surface roughness.

References

[1] Shilpa, M. K., & Yendapalli, V. (2022). Surface roughness estimation techniques for drilled Surfaces: A review. *Materials Today: Proceedings*, *52*, 1082–1091. https://doi.org/10.1016/j.matpr.2021.10.496

[2] Chen, S., Feng, R., Zhang, C., & Zhang, Y. (2018b). Surface roughness measurement method based on multi-parameter modeling learning. *Measurement*, *129*, 664–676. https://doi.org/10.1016/j.measurement.2018.07.071

[3] Chen, S., Feng, R., Zhang, C., & Zhang, Y. (2018). Surface roughness measurement method based on multi-parameter modeling learning. *Measurement*, *129*, 664–676. https://doi.org/10.1016/j.measurement.2018.07.071

[4] Huaian, Y. I., Jian, L., Lu, E., & Peng, A. (2016). Measuring grinding surface roughness based on the sharpness evaluation of colour images. *Measurement Science and Technology*, *27*(2), 025404. https://doi.org/10.1088/0957-0233/27/2/025404

[5] Yi, H., Liu, J., Peng, A., Lu, E., & Zhang, H. (2016). Visual method for measuring the roughness of a grinding piece based on color indices. *Optics Express*, *24*(15), 17215. https://doi.org/10.1364/oe.24.017215

[6] Liu, J., Lu, E., Yi, H., Wang, M., & Peng, A. (2017). A new surface roughness measurement method based on a color distribution statistical matrix. *Measurement*, *103*, 165–178. https://doi.org/10.1016/j.measurement.2017.02.036

[7] Lu, E., Liu, J., Gao, R., Yi, H., Wang, W., & Suo, X. (2018). Designing indices to measure surface roughness based on the color distribution statistical matrix (CDSM). *Tribology International*, *122*, 96–107. https://doi.org/10.1016/j.triboint.2018.02.033

[8] Rifai, A. P., Aoyama, H., Thọ, N. H., Dawal, S. Z. M., & Masruroh, N. A. (2020). Evaluation of turned and milled surfaces roughness using convolutional neural network. *Measurement*, *161*, 107860. https://doi.org/10.1016/j.measurement.2020.107860

[9] Saeedi, J., Dotta, M., Galli, A., Nasciuti, A., Maradia, U., Boccadoro, M., Gambardella, L. M., & Giusti, A. (2020). Measurement and inspection of electrical discharge machined steel surfaces using deep neural networks. *Machine Vision and Applications*, *32*(1). https://doi.org/10.1007/s00138-020-01142-w

[10] Tatzel, L., & León, F. P. (2020). Image-based roughness estimation of laser cut edges with a convolutional neural network. *Procedia CIRP*, *94*, 469–473. https://doi.org/10.1016/j.procir.2020.09.166

[11] Chen, Y., Yi, H., Liao, C., Huang, P., & Chen, Q. (2021). Visual measurement of milling surface roughness based on Xception model with convolutional neural network. *Measurement*, *186*, 110217. https://doi.org/10.1016/j.measurement.2021.110217

[12] Giusti, A., Dotta, M., Maradia, U., Boccadoro, M., Gambardella, L. M., & Nasciuti, A. (2020). Image-based Measurement of Material Roughness using Machine Learning Techniques. *Procedia CIRP*, *95*, 377–382. https://doi.org/10.1016/j.procir.2020.02.292

[13] Ibarra-Zárate, D. I., Alonso-Valerdi, L. M., Chuya-Sumba, J., Velarde-Valdez, S., & Siller, H. R. (2019). Prediction of Inconel 718 roughness with acoustic emission using convolutional neural network based regression. *The International Journal of Advanced Manufacturing Technology*, *105*(1-4), 1609–1621. https://doi.org/10.1007/s00170-019-04378-7

[14] Qi, J., Chen, B., & Zhang, D. (2020). Multi-information fusion-based belt condition monitoring in grinding process using the improved-Mahalanobis distance and convolutional neural networks. *Journal of Manufacturing Processes*, *59*, 302–315. https://doi.org/10.1016/j.jmapro.2020.09.061

[15] Sutton, M. A., Orteu, J., & Schreier, H. W. (2009). *Image correlation for shape, motion and deformation measurements*. Springer. https://doi.org/10.1007/978-0-387-78747-3

[16] Al-Kindi, G., & Shirinzadeh, B. (2007). An evaluation of surface roughness parameters measurement using vision-based data. *International Journal of Machine Tools & Manufacture*, *47*(3-4), 697–708. https://doi.org/10.1016/j.ijmachtools.2006.04.013

[17] Guo, R., & Zhang, T. (2011). Experimental investigation of a modified Beckmann–Kirchhoff scattering theory for the in-process optical measurement of surface quality. *Optik*, *122*(21), 1890–1894. https://doi.org/10.1016/j.ijleo.2010.11.019

[18] Omiotek, Z., & Kotyra, A. (2021). Flame image processing and classification using a Pre-Trained VGG16 model in combustion diagnosis. *Sensors*, *21*(2), 500. https://doi.org/10.3390/s21020500

[19] Zu, D., Zhang, F., Wu, Q., Wang, W., Yang, Z., & Hu, Z. (2022). Disease identification of Lentinus edodes sticks based on deep learning model. *Complexity*, *2022*, 1–9. https://doi.org/10.1155/2022/9504055

[20] Bowd, C., Belghith, A., Zangwill, L. M., Christopher, M., Goldbaum, M. H., Fan, R., Rezapour, J., Moghimi, S., Kamalipour, A., Hou, H., & Weinreb, R. N. (2022). Deep learning image analysis of optical coherence tomography angiography measured vessel density improves classification of healthy and glaucoma eyes. *American Journal of Ophthalmology*, *236*, 298–308. https://doi.org/10.1016/j.ajo.2021.11.008

Jiefeng Huang is a postgraduate student in the College of Mechanical and Control Engineering at Guilin University of Technology. His main research area is machine vision.

Huaian Yi is an associate professor in the College of Mechanical and Control Engineering at Guilin University of Technology., His main research area is machine vision.

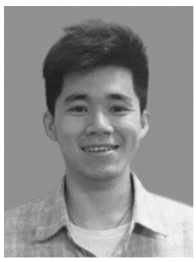

Runji Fang received his B.S. degree from Guilin University of Technology in 2020. At present, he is a graduate of Guilin University of Technology. His main research interest is machine vision.

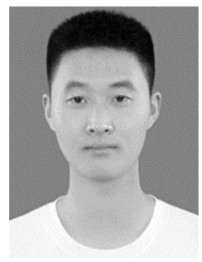

Kun Song is a postgraduate student at the College of Mechanical and Control Engineering at Guilin University of Technology. His main research area is binocular vision.